Denitrification-driven transcription and enzyme production at the river–groundwater interface: Insights from reactive-transport modeling

Anna Störiko[1,1], Holger Pagel[2,2], Adrian Mellage[1,1], Philippe Van Cappellen[3,3], and Olaf A. Cirpka[1,1]

[1]University of Tübingen
[2]University of Hohenheim
[3]University of Waterloo

November 30, 2022

Abstract

The interface between rivers and groundwater is a key driver for the turnover of reactive nitrogen compounds, that cause eutrophication of rivers and endanger drinking-water production from groundwater. Molecular-biological data and omics tools have been used to characterize microorganisms responsible for the turnover of nitrogen compounds. While transcripts of functional genes and enzymes are used as measures of microbial activity it is not yet clear how they quantitatively relate to actual turnover rates under variable environmental conditions. We developed a reactive-transport model for denitrification that simultaneously predicts the distributions of functional-gene transcripts, enzymes and reaction rates. Applying the model, we evaluate the response of transcripts and enzymes at the river–groundwater interface to stable and dynamic hydrogeochemical regimes. While functional-gene transcripts respond to short-term (diurnal) fluctuations of substrate availability and oxygen concentrations, enzyme concentrations are stable over such time scales. The presence of functional-gene transcripts and enzymes globally coincides with the zones of active denitrification. However, transcript and enzyme concentrations do not directly translate into denitrification rates in a quantitative way because of non-linear effects and hysteresis caused by variable substrate availability and oxygen inhibition. Based on our simulations, we suggest that molecular-biological data should be combined with aqueous chemical data, which can typically be obtained at higher spatial and temporal resolution, to parameterize and calibrate reactive-transport models.

Denitrification-driven transcription and enzyme production at the river–groundwater interface: Insights from reactive-transport modeling

Anna Störiko[1], Holger Pagel[2], Adrian Mellage[1], Philippe Van Cappellen[3]and Olaf A. Cirpka[1]

[1]Center for Applied Geoscience, University of Tübingen, Tübingen, Germany
[2]Biogeophysics, Institute of Soil Science and Land Evaluation, University of Hohenheim, Stuttgart, Germany
[3]Water Institute, Department of Earth and Environmental Sciences, University of Waterloo, Waterloo, Ontario, Canada

Key Points:

- We simulate the distributions of functional-gene transcripts and enzymes related to denitrification at the river–groundwater interface
- Functional-gene transcripts respond quickly to diurnal fluctuations of substrate and oxygen concentrations
- Substrate limitation and oxygen inhibition impede the direct prediction of denitrification rates from transcript or enzyme concentrations

Corresponding author: Anna Störiko, anna.stoeriko@uni-tuebingen.de

Corresponding author: Olaf Cirpka, olaf.cirpka@uni-tuebingen.de

Abstract

The interface between rivers and groundwater is a key driver for the turnover of reactive nitrogen compounds, that cause eutrophication of rivers and endanger drinking-water production from groundwater. Molecular-biological data and omics tools have been used to characterize microorganisms responsible for the turnover of nitrogen compounds. While transcripts of functional genes and enzymes are used as measures of microbial activity it is not yet clear how they quantitatively relate to actual turnover rates under variable environmental conditions. We developed a reactive-transport model for denitrification that simultaneously predicts the distributions of functional-gene transcripts, enzymes and reaction rates. Applying the model, we evaluate the response of transcripts and enzymes at the river–groundwater interface to stable and dynamic hydrogeochemical regimes. While functional-gene transcripts respond to short-term (diurnal) fluctuations of substrate availability and oxygen concentrations, enzyme concentrations are stable over such time scales. The presence of functional-gene transcripts and enzymes globally coincides with the zones of active denitrification. However, transcript and enzyme concentrations do not directly translate into denitrification rates in a quantitative way because of non-linear effects and hysteresis caused by variable substrate availability and oxygen inhibition. Based on our simulations, we suggest that molecular-biological data should be combined with aqueous chemical data, which can typically be obtained at higher spatial and temporal resolution, to parameterize and calibrate reactive-transport models.

Plain Language Summary

Nitrate inputs, including from agricultural fertilizer applications, threaten groundwater quality and drinking water production. In the process of denitrification, bacteria can remove nitrate by converting it into harmless nitrogen gas using specialized enzymes. The interface between rivers and groundwater is a known hotspot for denitrification. Molecular-biological tools can detect how many enzymes, functional genes, and gene-transcripts (i.e., precursors of enzyme production) associated with denitrification exist in a sample. Although these measurements contain valuable information about the number of bacteria and how active they are, their exact relationships with the denitrification rate and thus nitrate removal remain unclear. Here, we use a computational model to simulate the coupled dynamics of denitrification, bacteria, transcripts, and enzymes when nitrate-rich groundwater interacts with a nearby river. The simulations yield complex and non-unique relationships between the denitrification rates and the molecular-biological variables. While functional-gene transcripts respond to daily fluctuations of environmental conditions, enzyme concentrations and genes are stable over such time scales. High levels of functional-gene transcripts therefore provide a good qualitative indicator of reactive zones. Quantitative predictions of nitrate turnover, however, will require high-resolution measurements of the reacting compounds, genes, and transcripts.

1 Introduction

The increase of diffuse nitrogen inputs, mainly by agriculture, has led to elevated concentrations of reactive-nitrogen species in groundwater and surface-water bodies, threatening drinking-water production, and causing eutrophication of rivers and lakes (Erisman et al., 2013). Microorganisms use reactive nitrogen compounds as substrates for redox reactions that fuel their energy metabolism, constituting the main attenuation process for nitrogen contamination in environmental systems (Kuypers et al., 2018). Understanding the factors that foster microbial removal of reactive nitrogen species from the environment is therefore critical for contamination control and mitigation. Denitrification is the key reaction for the permanent removal of nitrogen species from the environment because it converts the reactive-nitrogen species nitrate into inert N_2 gas rather than into another reactive-nitrogen species. The interface between surface waters and groundwater plays a key role for the

turnover of nitrogen compounds because steep redox gradients (from oxic rivers to anoxic groundwater) and the availability of labile organic carbon as an electron donor, either in the river water or in the hyporheic and riparian zones, enhance microbial reactions (Krause et al., 2011, 2017).

Molecular-biological tools and so-called omics techniques, i.e., (meta)genomics, (meta-)transcriptomics, (meta)proteomics analyses, have been used to characterize microbial nitrogen cycling in riparian zones (Wang et al., 2019), lake and river sediments (Stoliker et al., 2016; Reid et al., 2018), and the hyporheic zone (Danczak et al., 2016) by providing information about the microbial community composition, its functional and metabolic potential, and activity. While these methods can help to identify the relevant processes at a particular site and outline reactive zones, it remains a challenge to quantitatively relate molecular-biological measurements to turnover rates of nitrogen. Meta-omics data primarily target the relative (qualitative) abundance of genes, transcripts, and proteins and are particularly difficult to convert into rate expressions. In contrast, measurements of functional genes, their transcripts, and the corresponding enzymes directly relate to the abundance of organisms capable of specific metabolic pathways and their activity. Several studies have suggested using transcript levels or transcript-to-gene ratios to estimate reaction rates of contaminant (Rahm & Richardson, 2008; Brow et al., 2013), pesticide (Monard et al., 2013) or nitrogen-species turnover (Rohe et al., 2020). However, there is still a need to investigate if and under which conditions molecular-biological information can serve as a proxy for reaction rates, particularly in spatially variable and temporally dynamic environmental systems.

The river–groundwater interface is a very dynamic environmental system, exhibiting temporal variability on scales ranging from diurnal cycles (e.g., oxygen and temperature) via individual events to seasonal variations of temperature, discharge, and nutrient/substrate loading. Natural dynamics are superimposed by anthropogenic dynamics such as diurnal river-stage fluctuations in managed river systems affected by hydropower, so-called hydropeaking (Sawyer et al., 2009). These dynamics drive highly dynamic spatial and temporal biogeochemical turnover, underscoring the importance of understanding the impact of such forcings on (molecular biological) variables of interest. Spatially and temporally highly resolved measurements of gene, transcript, or enzyme concentrations are usually not feasible because each sample provides information only about a single point in space and time, and the costs are very high. Process-based modeling may help to bridge between a limited number of molecular-biological measurements, continuously logged physical and chemical parameters (e.g., using probes), and the need to understand the system's biological, chemical, and physical functioning at scales relevant for management. This requires reliable models of microbially mediated turnover and solute transport that can simulate molecular-biological data.

In a preceding study, we developed a gene-based, enzyme-explicit model of denitrification, and calibrated it with results from a batch incubation experiment (Störiko et al., 2021a). In the present study, we extend the model to account for advective-dispersive transport and use it to predict the patterns of functional-gene-transcript and enzyme concentrations for several scenarios of denitrification at the river–groundwater interface. In particular, we explore the expected molecular-biological signature of denitrification (functional-gene transcripts and enzymes) at the river–groundwater interface. Furthermore, we relate model-computed denitrification rates to simulated concentrations of transcripts and enzymes over time and space. Based on our results, we probe the type of potential sampling schemes that would yield reliable estimates of overall nitrogen turnover, and the conditions needed to derive simple functional relationships between quantitative molecular-biological measurements and reaction rates. Our modeling study provides guidelines regarding the interpretability of molecular-biological and omics measurements, collected in field investigations that aim to capture nitrogen turnover at the river–groundwater interface.

2 Methods

2.1 Model Scenarios

We set up three model scenarios that represent different hydrological conditions at the river–groundwater interface (Figure 1), ranging from steady-state hydrology and biogeochemistry to pronounced diurnal cycles. In all scenarios, we considered microbial aerobic respiration and denitrification. Both pathways were coupled to the oxidation of dissolved organic carbon (DOC) which was provided via hydrolysis of particulate organic carbon (POC) in the aquifer matrix and via inflow from the river water.

The first scenario simulated constant groundwater discharge (GD), where nitrate-rich water from the aquifer recharged into the river (Figure 1a), a common situation in agricultural landscapes. In addition, we assumed that the reactive POC concentration was highest near the river and decreased with increasing distance away from the streambed. That is, we imposed a gradient in the electron donor availability that focused the denitrification activity near the river-aquifer interface. The formulation of the gradient is presented in the next section (see equations 11 and 12).

In the second scenario, we simulated oxic river water continuously entering the aquifer (Figure 1b), mimicking a bank-filtration (BF) scenario that could be either induced by pumping or by the natural hydraulic gradient of the system. Oxygen concentrations in river water can be subject to strong daily fluctuations, reflecting the interplay between radiation-dependent photosynthesis, aerobic respiration, and gas exchange in the river (Hayashi et al., 2012; Kunz et al., 2017). We considered two sub-scenarios: In the first, the oxygen concentration in the river remained at a constant level of $8\,\mathrm{mg\,L^{-1}}$ (BFC, constant oxygen), whereas in the second the concentration sinusoidally fluctuated about the mean value, yielding dynamic redox conditions close to the river–groundwater interface (BFP, periodic oxygen).

In a third scenario, denoted bank storage (BS), we considered a flow-reversal, induced by dynamic river-stage fluctuations, reflecting hydropeaking or tidal influences (Figure 1c). Close to the river–groundwater interface, the flow reversal caused alternating oxic and anoxic conditions.

2.2 Governing Equations

2.2.1 Advective-Dispersive-Reactive Transport

We described transport and reaction of dissolved compounds (nitrate, nitrite, oxygen, DOC) via the one-dimensional (1-D) advection-dispersion-reaction equation. The evolution of compound i's concentration c_i in space (x) and time (t) is thus given by:

$$\frac{\partial c_i}{\partial t} + v\frac{\partial c_i}{\partial x} - D\frac{\partial^2 c_i}{\partial x^2} = r^i_{\mathrm{net}}\,, \tag{1}$$

where v [$\mathrm{m\,s^{-1}}$] is the average linear flow velocity, D [$\mathrm{m^2\,s^{-1}}$] is the dispersion coefficient, and r^i_{net} is the net reaction rate of compound i. We used the parametrization of Scheidegger (1974) for dispersion:

$$D = |v|\alpha_L + D_e\,, \tag{2}$$

where α_L [m] is the longitudinal dispersivity and D_e [$\mathrm{m^2\,s^{-1}}$] denotes the pore-diffusion coefficient. We further assumed that flow is at quasi-steady state, in which v is uniform in space and reacts instantaneously to changes in boundary conditions. In scenarios GD and BF, the velocity is constant in time, whereas in scenario BS, we approximated v as a sinusoidal function of time with mean velocity $\bar{v}$ [$\mathrm{m\,s^{-1}}$], amplitude $\hat{v}$ [$\mathrm{m\,s^{-1}}$] and frequency f_v [$\mathrm{s^{-1}}$]:

$$v(t) = \bar{v} + \hat{v}\sin(2\pi f_v t) \tag{3}$$

In all simulations we neglected transport of bacterial cells because the majority (more than 99 % according to Griebler et al., 2002) of active microorganisms in the subsurface are attached

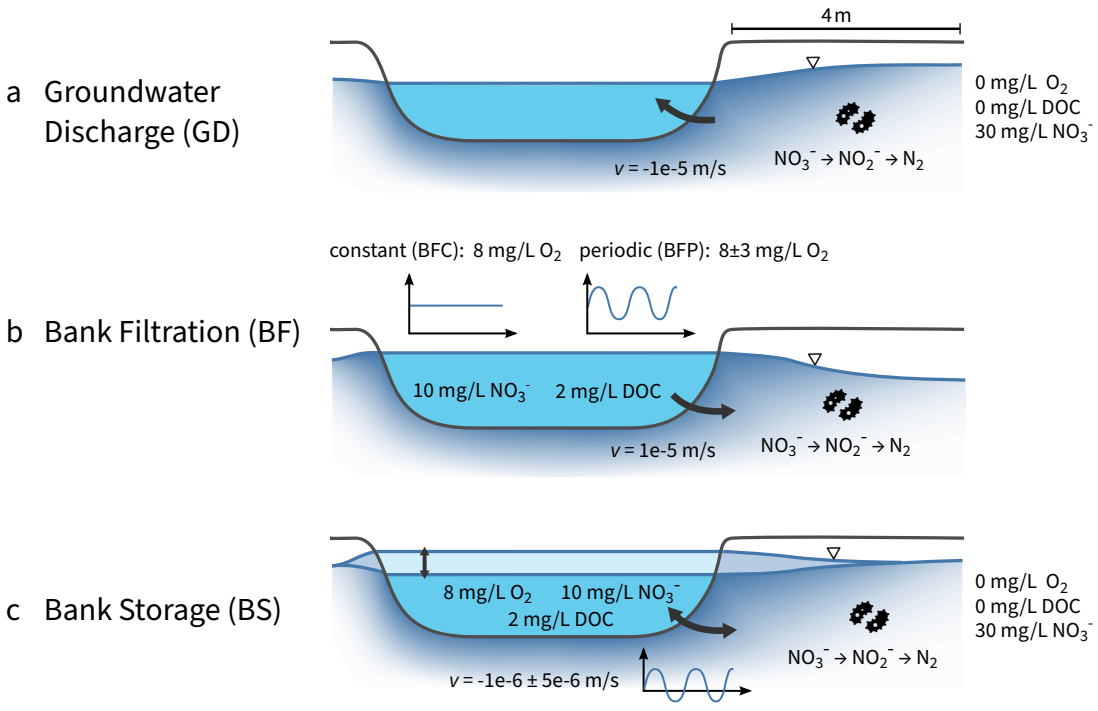

Figure 1. Schematic of the three simulation scenarios and the corresponding boundary conditions.

to sediments (Smith et al., 2018). Transcripts and enzymes were assumed to be confined to the interior of bacterial cells and thus to be immobile.

2.2.2 Microbial Reactions

We used an enzyme-based model formulation of microbial denitrification (Störiko et al., 2021a) that reflects the biological regulation of reaction rates by simulating concentrations of transcription factors, functional-gene transcripts, and enzymes explicitly. The reaction model describes both aerobic respiration and reduction of nitrate to N_2 via NO_2^- as a reactive intermediate. Denitrification is coupled to the oxidation of organic carbon, formally expressed as succinate, serving as an electron donor and carbon source for the facultative anaerobe *Paracoccus denitrificans*. Herein, we applied the parameters in Störiko et al. (2021a) specific to *P. denitrificans* to simulate denitrification coupled to DOC oxidation (assuming that succinate acts as a generalized form of DOC) to the flow scenarios outlined in Figure 1. Despite the parameters being specific to a pure-culture batch experiment (Qu et al., 2015), they provide an opportunity with which to probe the thus far poorly-characterized behavior of transcription and enzyme regulation in natural subsurface-transport settings, relevant for biogeochemical laboratory and field investigations. In the following we briefly summarize key model processes and refer the reader to the original publication for more detail.

The catabolic reactions were described by the following stoichiometric equations:

$$7\,NO_3^- + C_4H_6O_4 \xrightarrow{narG} 7\,NO_2^- + 4\,CO_2 + 3\,H_2O \tag{4}$$

$$14\,NO_2^- + 14\,H^+ + 3\,C_4H_6O_4 \xrightarrow{nirS} 7\,N_2 + 12\,CO_2 + 16\,H_2O \tag{5}$$

$$7\,O_2 + 2\,C_4H_6O_4 \longrightarrow 8\,CO_2 + 6\,H_2O \tag{6}$$

Gene expression is controlled by the transcription factors FnrP, sensitive to oxygen levels, NarR, regulated by nitrate and nitrite, and NNR, stimulated in the presence of nitrite and

absence of oxygen. Transcription of the *narG* gene, coding for nitrate reductase (NAR), is initiated in the presence of FnrP and NarR, whereas the transcription of *nirS*, coding for nitrite reductase (NIR), requires NNR. The concentrations of transcripts were assumed to be at quasi-steady state with the transcription factor concentrations. The NAR and NIR enzymes are produced in response to *narG* and *nirS* levels and decay following a first-order rate.

Denitrification rates are a function of the enzyme concentrations, a double Michaelis-Menten term for the limitation of electron donor (DOC) and electron acceptor (nitrate, nitrite) concentrations and an oxygen inhibition term:

$$r_N = k^j_{\max} E_j \frac{c_N}{K_N + c_N} \frac{c_{\mathrm{DOC}}}{K_{\mathrm{DOC}} + c_{\mathrm{DOC}}} \frac{I^j_{\mathrm{O}_2}}{c_{\mathrm{O}_2} + I^j_{\mathrm{O}_2}} \tag{7}$$

Here, $k^j_{\max}$ [s^{-1}] is the amount of substrate that the enzyme j (NAR or NIR) can maximally turn over per time (also called turnover number), E_j is the concentration of enzyme j that catalyzes the reaction of substrate N (nitrate or nitrite). K_N [$\mathrm{mol\,L^{-1}}$] and K_{DOC} [$\mathrm{mol\,L^{-1}}$] are the half-saturation concentrations for nitrate/nitrite and DOC, respectively, and $I^j_{\mathrm{O}_2}$ [$\mathrm{mol\,L^{-1}}$] is the oxygen inhibition constant for enzyme j. Aerobic respiration was described by a standard double Michaelis-Menten formulation with the maximum cell-specific respiration rate $v^{\mathrm{O}_2}_{\max}$ [$\mathrm{mol\,cell^{-1}\,s^{-1}}$] and biomass concentration B [$\mathrm{cells\,L^{-1}}$]:

$$r_{\mathrm{O}_2} = v^{\mathrm{O}_2}_{\max} B \frac{c_{\mathrm{O}_2}}{K_{\mathrm{O}_2} + c_{\mathrm{O}_2}} \frac{c_{\mathrm{DOC}}}{K_{\mathrm{DOC}} + c_{\mathrm{DOC}}} \tag{8}$$

To predict the dynamics of transcripts and enzymes under conditions similar to those found in natural environments, we modified and complemented the parts of the model that relate to DOC and biomass. (Note: in our original formulation carbon was assumed to be non-limiting). Here, the model was expanded to include the release of DOC from POC in the aquifer matrix, and its consumption by both denitrification and aerobic respiration. The latter yielded a DOC consumption dependent on the electron-acceptor consumption rates (defined in equations 7 and 8) and their stoichiometric coefficients in the metabolic reaction:

$$r^j_{\mathrm{DOC}} = \frac{\gamma^i_{DOC}}{\gamma^j_A} r^j_A \tag{9}$$

and

$$r_{\mathrm{DOC}} = \sum_j r^j_{\mathrm{DOC}}\,, \tag{10}$$

where γ^j_A and γ^j_{DOC} are the stoichiometric coefficients of the electron acceptor and DOC in reaction (j) and r^j_A is the corresponding electron-acceptor reaction rate. We modeled the release of DOC from the POC-containing aquifer matrix as a first-order mass transfer process (Kinzelbach et al., 1991; Gu et al., 2007; Knights et al., 2017), with the first-order coefficient $k^{\mathrm{DOC}}_{\mathrm{release}}$ [1/s]:

$$r_{\mathrm{release}} = k^{\mathrm{DOC}}_{\mathrm{release}} \left(c^{\mathrm{sat}}_{\mathrm{DOC}} - c_{\mathrm{DOC}} \right) \tag{11}$$

The DOC saturation concentration $c^{\mathrm{sat}}_{\mathrm{DOC}}$ [$\mathrm{mol\,L^{-1}}$] depends on the POC content of the sediment, which tends to decrease with distance from the river (Marmonier et al., 1995; Stelzer et al., 2011). Following Knights et al. (2017), we therefore assumed an exponential profile of $c^{\mathrm{sat}}_{\mathrm{DOC}}$:

$$c^{\mathrm{sat}}_{\mathrm{DOC}} = c^{\mathrm{sat},0}_{\mathrm{DOC}} \exp\left(-\frac{x}{l}\right)\,, \tag{12}$$

where l [m] is the length scale for the concentration decrease.

In contrast to the original formulation, bacterial growth was parameterized as a function of the oxidation of organic carbon coupled to both oxygen and nitrogen oxide reduction.

The synthesis of biomass, represented with the molecular formula $C_{10}H_{18}O_5N_2$, can formally be described by the reaction:

$$3\,C_4H_6O_4 + 2\,NH_4^+ \longrightarrow C_{10}H_{18}O_5N_2 + 2\,CO_2 + 3\,H_2O + 2\,H^+ \tag{13}$$

Equation 13 was then coupled to the energy-gaining reactions 4–6 to obtain the overall metabolic reaction. The stoichiometric coefficients in the metabolic reaction depend on the number of catabolic formula reactions that must be completed to generate the energy required for one anabolic formula reaction (and thus produce one mol of biomass). In turn, this number is directly related to the growth yield Y_i [cells $\mathrm{mol_C^{-1}}$], which corresponds to the amount of biomass that is produced per mole of organic carbon consumed. The growth yield relates the growth rate associated to the electron acceptor i to the corresponding DOC-consumption rate:

$$r^i_{\mathrm{growth}} = Y_i r^i_{\mathrm{DOC}} \tag{14}$$

Furthermore, we applied a logistic term to the biomass-growth expression (not to the substrate consumption rates) to limit biomass growth to a set maximum density (e.g., Grösbacher et al., 2018). This is in line with observations that biomass densities in porous media reach a "carrying capacity", even under non-growth-limiting conditions (Mellage et al., 2015; Ding, 2010). The logistic growth term can be interpreted as a reduction in the maximum growth yield by the occupancy level:

$$Y_i = Y^i_{\mathrm{max}} \left(1 - \frac{B}{B_{\mathrm{max}}}\right), \tag{15}$$

where Y^i_{max} is the maximum growth yield and B_{max} is the carrying capacity. This implies that the growth yield and therefore the stoichiometric coefficients of the metabolic reactions depend on the biomass concentration. The model also accounts for biomass decay via a first-order term with the decay coefficient k_{dec} [$\mathrm{s^{-1}}$]:

$$r_{\mathrm{decay}} = k_{\mathrm{dec}} B \tag{16}$$

This leads to the build-up of dead biomass, which, in turn, decays in a first-order process with constant k_{min}, releasing DOC via mineralization.

2.2.3 Boundary Conditions

Fixed concentration (Dirichlet) boundary conditions were applied at the river and groundwater inflow boundaries. The river water was assumed to be saturated with respect to oxygen, and contained $10\,\mathrm{mg\,L^{-1}}$ of nitrate and $2\,\mathrm{mg\,L^{-1}}$ of DOC. These concentrations correspond to anthropogenically influenced but not excessively nutrient-enriched rivers. The inflowing groundwater was assumed to be anoxic but rich in nitrate ($30\,\mathrm{mg\,L^{-1}}$) and depleted in DOC. In scenario BFP, oxygen concentrations in the river were described by a sinusoidal function with amplitude $\widehat{c_{\mathrm{O_2}}}$ [$\mathrm{mol\,L^{-1}}$], frequency $f_{\mathrm{O_2}} = 1\,\mathrm{d^{-1}}$ and mean value $\overline{c_{\mathrm{O_2}}}$ [$\mathrm{mol\,L^{-1}}$]:

$$c^{\mathrm{in}}_{\mathrm{O_2}}(t) = \widehat{c_{\mathrm{O_2}}} \sin\left(2\pi f_{\mathrm{O_2}} t\right) + \overline{c_{\mathrm{O_2}}} \tag{17}$$

All other concentrations at the inflow boundary were constant over time, with values given in Table 1. At the outflow boundary, we assumed zero dispersive flux.

2.3 Simulation Parameters

Parameters related to transcript and enzyme concentrations, denitrification and aerobic respiration were obtained from our previous study (Störiko et al., 2021a) in which we calibrated the enzyme-based model with the laboratory data of Qu et al. (2015). In the simulations presented here, the median values of the parameter distributions in Störiko et al. (2021a) were imposed (Table 1). Values of new parameters, that is, those that were not included in the previous model (transport and DOC-related parameters) were chosen based on literature values.

Table 1. Parameter values used in the simulation.

Parameter	Description	Value	Unit	Reference
v	linear velocity (GD, BF)	10^{-5}	$\mathrm{m\,s^{-1}}$	a
$\bar{v}$	mean velocity (BS)	-10^{-6}	$\mathrm{m\,s^{-1}}$	b
$\hat{v}$	velocity amplitude (BS)	10^{-5}	$\mathrm{m\,s^{-1}}$	b
f_v	velocity frequency (BS)	1	$\mathrm{d^{-1}}$	c
α_L	longitudinal dispersivity	0.1	m	d
D_e	effective diffusion coefficient	3×10^{8}	$\mathrm{m^2\,s^{-1}}$	e
$k_{\max}^{NO_3^-}$	NAR turnover number	4.4×10^{4}	$\mathrm{s^{-1}}$	f
$k_{\max}^{NO_2^-}$	NIR turnover number	2.9×10^{2}	$\mathrm{s^{-1}}$	f
$K_{NO_3^-}$	NO_3^- half-saturation constant	5	µM	g
$K_{NO_2^-}$	NO_3^- half-saturation constant	5	µM	g
K_{DOC}	DOC half-saturation constant	40	$\mathrm{\mu mol_C\,L^{-1}}$	h
$I_{O_2}^{\mathrm{NAR}}$	O_2 inhibition constant for NAR	1	µM	f
$I_{O_2}^{\mathrm{NIR}}$	O_2 inhibition constant for NIR	340	nM	f
$v_{\max}^{O_2}$	maximum cell-specific O_2 oxidation rate	6.4×10^{-19}	$\mathrm{mol\,cell^{-1}\,s^{-1}}$	f
K_{O_2}	O_2 half-saturation constant	31	µM	f
$k_{\mathrm{release}}^{\mathrm{DOC}}$	DOC release rate constant	0.2	$\mathrm{d^{-1}}$	i
$c_{\mathrm{DOC}}^{\mathrm{sat},0}$	maximum DOC saturation concentration	20.8	$\mathrm{mmol_C\,L^{-1}}$	j
l	length scale for decrease in sediment POC	0.2	m	k
$Y_{\max}^{NO_3^-}$	maximum growth yield with NO_3^-	2.6×10^{13}	$\mathrm{cells\,mol_C^{-1}}$	l
$Y_{\max}^{NO_2^-}$	maximum growth yield with NO_2^-	1.6×10^{13}	$\mathrm{cells\,mol_C^{-1}}$	l
$Y_{\max}^{O_2}$	maximum growth yield with O_2	7.7×10^{13}	$\mathrm{cells\,mol_C^{-1}}$	f, m
$B_{\max}$	carrying capacity	3.3×10^{11}	$\mathrm{cells\,L^{-1}}$	n
k_{dec}	biomass decay constant	10^{-7}	$\mathrm{s^{-1}}$	o
$c_{O_2}^{\mathrm{in}}$	O_2 concentration in the river (GD, BFC, BS)	250	µM	p
$\overline{c_{O_2}}$	mean O_2 concentration in the river (BFP)	250	µM	p
$\widehat{c_{O_2}}$	amplitude of oxygen fluctuations (BFP)	94	µM	q
$c_{NO_3^-}^{\mathrm{river}}$	NO_3^- concentration in the river	161	µM	r
$c_{NO_3^-}^{\mathrm{GW}}$	NO_3^- concentration in groundwater	484	µM	r
$c_{\mathrm{DOC}}^{\mathrm{river}}$	DOC concentration in the river	167	$\mathrm{\mu mol_C\,L^{-1}}$	s

[a] See Bertin and Bourg (1994) for bank filtration and Kennedy et al. (2009) for groundwater exfiltration. [b] Gerecht et al. (2011); Liu et al. (2017) [c] Diurnal cycles. [d] Gelhar et al. (1992) [e] Based on the approximation $D_e = D\theta$ where $D = 10^{-9}\,\mathrm{m^2\,s^{-1}}$ is the molecular diffusion coefficient and $\theta = 0.3$ is porosity. [f] Median of the parameters in Störiko et al. (2021a). [g] Hassan et al. (2016) [h] Fixed to a value within reported ranges (Sanz-Prat et al., 2016; Kinzelbach et al., 1991). [i] Fixed to a value within reported ranges (Sanz-Prat et al., 2016; Kinzelbach et al., 1991; Gu et al., 2007; Sawyer, 2015). [j] Fixed to a value within reported ranges (Gu et al., 2007; Sawyer, 2015; Kinzelbach et al., 1991). [k] Knights et al. (2017) [l] Fixed to a value within reported ranges (Hassan et al., 2016, 2014). [m] Value corrected for the incorporation of organic carbon into biomass, which was not considered in Störiko et al. (2021a). [n] Fixed to a value within reported ranges (Ding, 2010). [o] Fixed to a value within reported ranges (Ding, 2010; Kinzelbach et al., 1991). [p] Liu et al. (2017) [q] Kunz et al. (2017) [r] Gu et al. (2007); Liu et al. (2017) [s] Hayashi et al. (2012); Bol et al. (2015)

2.4 Numerical Methods

We used the cell-centered finite volume method to discretize the reactive-transport equation 1 in space, applying a first-order upwind scheme for advection. The domain had a total length of 4 m and was divided into 200 cells with a uniform spacing of 2 cm. The resulting system of ordinary differential equations (ODEs) was solved with the backwards differentiation formula (BDF) as implemented in the CVODES solver in the SUNDIALS library (Hindmarsh et al., 2005). All code was written in Python 3.8, and the package Sunode (Seyboldt, 2021) that wraps CVODES was used for solving the ODEs. The simulations were run until reaching steady state (in the scenarios with constant boundary conditions) or dynamic steady state, that is, self repeating time cycles in the scenarios with periodic boundary conditions.

3 Results & Discussion

3.1 Zonation of Redox Species and Denitrifying Bacteria

The three model scenarios result in distinct spatial distributions of N species, transcripts, enzymes, biomass, oxygen and DOC (Figure 2, rows a–f). In the following we present and discuss the predicted steady-state concentrations scenario-wise in detail: GD (Figure 2, left column), BF (Figure 2, center column) and BS (Figure 2, right column).

3.1.1 Scenario GD: Groundwater Discharge

Nitrate enters the domain with in-flowing groundwater, and remains at high concentrations (i.e., close to the inflow value) over the first 2 m of the domain, where the aquifer matrix contains only little POC (electron donor limitation). At about 1.5 m from the river, nitrate begins to drop and is completely depleted at a distance of 0.25 m from the sediment-river interface. Nitrite concentrations increase, mirroring the drop in nitrate, until reaching a peak value of 340 $\mu mol\,L^{-1}$ at 0.3 m and then decrease towards the river. Our model-predicted nitrite concentrations are higher than typically observed in natural sediments. Profiles of porewater nitrite in several studies indicate that the concentrations are usually below 30 $\mu mol\,L^{-1}$ (Akbarzadeh et al., 2018; Stief et al., 2002; Harvey et al., 2013). The parameter set used here is based on laboratory batch experiments with a single strain where strong nitrite accumulation was observed (Störiko et al., 2021a). Thus, while the high model-derived nitrite concentrations may be specific to the strain used in the experiments, we assume that the spatial trends in nitrogen species consumption and production are likely generalizable. The concentration of DOC drops from 280 $\mu mol_C\,L^{-1}$ at the sediment-river interface to below 40 $nmol_C\,L^{-1}$ within 30 cm, driven by the prescribed exponentially decreasing content of POC in the sediment (the only source of DOC) away from the river boundary. The zones of nitrate and nitrite consumption coincide with elevated absolute concentrations of *narG* and *nirS* transcripts (that is, in units of transcripts L^{-1}) and NAR/NIR enzymes (Figure 2c, left column). In contrast, cell-specific *narG* transcript and NAR enzyme concentrations are high in the DOC-limited section of the domain, despite the absence of denitrification (Figure S1). Nitrate triggers transcription but the low availability of the electron donor (DOC) results in low biomass concentrations strongly limiting denitrification. High biomass concentrations are only reached close to the river, where denitrification activity is the highest.

3.1.2 Scenario BF: Bank Filtration

The center column in Figure 2 shows the dynamics of the two bank-filtration scenarios with periodic (BFP) and constant (BFC) oxygen concentrations in the inflow. In the BFP scenario, concentrations do not reach a steady state but concentration time series converge to repeating diurnal cycles.

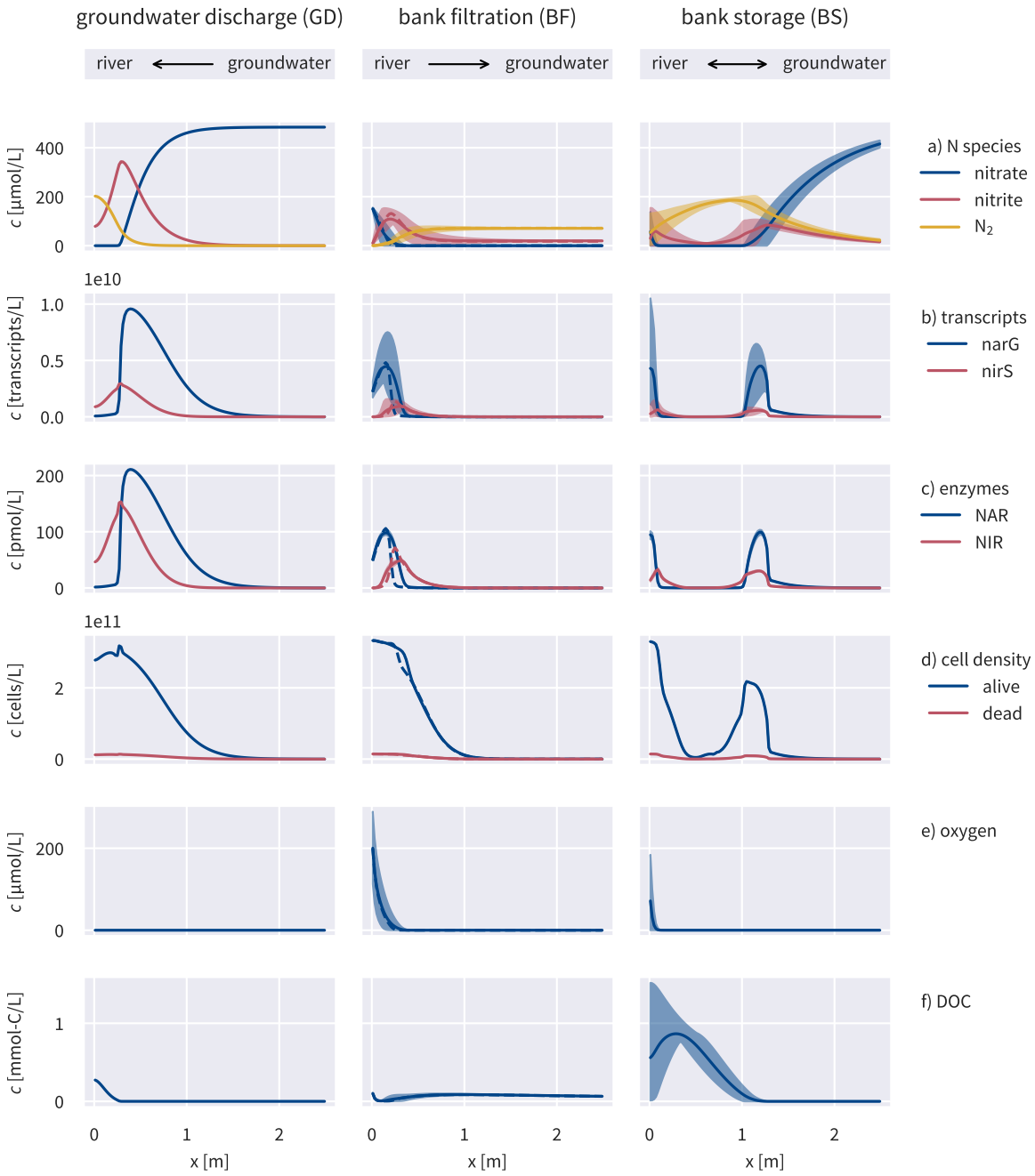

Figure 2. Spatial distributions of nitrogen compounds (a), transcript (b) and enzyme (c) concentrations, biomass (d), oxygen (e), and DOC (f) in the different scenarios. The steady-state solution in scenario BFC is indicated by a dashed line. For the periodic solution in scenarios BFP and BS, the minimum and maximum values over time are indicated by the shaded area, the mean value is plotted as a solid line. Concentrations between 2.5 m and the groundwater-side domain boundary at 4 m are omitted because they are almost constant.

The model predicts a zonation of the redox processes starting with aerobic respiration at the inflow boundary, where oxygen-rich river water infiltrates. Nitrate, present in the incoming water, is subsequently reduced to nitrite and N_2. The fluctuating oxygen concentrations in the river (inflow) in scenario BFP leads to a periodic shift in the location of the denitrification zone, which oscillates back and forth over 0.1 m about 0.2 m. At a given location, nitrate and nitrite concentrations fluctuate considerably over the course of the day. For example, nitrate concentrations at 0.2 m vary between 60 µmol L^{-1} and total depletion. Nitrite is reduced to low, but non-zero "residual" concentrations (20 µmol L^{-1}). The low concentration front subsequently penetrates deep into the aquifer. Biomass concentrations are very stable over time in the scenario with a fluctuating inflow oxygen concentration and hardly differ from the steady-state scenario. Cell doubling times in the simulations range from a few hours to several days, which is in accordance with literature values (Mailloux & Fuller, 2003). Similarly, biomass decay is slow (with a half-life of about 80 d, see Table 1), such that the biomass does not respond to daily cycles of substrate availability. Biomass concentrations are highest at the river inflow boundary where neither oxygen nor DOC are limiting and cell densities reach the maximum capacity $B_{\max}$. At locations where oxygen and nitrate are consumed, the remaining low nitrite concentrations can only sustain the survival of a small biomass pool (starting at 1.3 m from the river boundary), which in turn reduces the denitrification rate to values close to zero.

Transcripts of the *narG* gene are abundant in the region where nitrate is available and *nirS* transcripts co-occur with nitrite. In the scenario with dynamic boundary conditions, the transcript concentrations of denitrification genes exhibit a distinct diurnal cycle with an amplitude of up to 70 % (*narG*) and 100 % (*nirS*) of the mean value, in some parts of the domain. Concentrations of NAR and NIR enzymes follow the patterns of *narG* and *nirS* transcripts, but are much more dampened, with amplitudes that are one order of magnitude smaller than those of the corresponding transcripts. This difference stems from the different time scales of production and decay of transcript and enzymes. While transcripts usually decay within a few minutes (Bernstein et al., 2002; Härtig & Zumft, 1999) and are therefore assumed to be at quasi-steady state in our simulations, enzyme half-lives range on the order of several hours to days (Maier et al., 2011).

Because of the high DOC concentration (0.1 mmol L^{-1}) imposed at the river boundary, the river water serves as a DOC source. The DOC concentration, however, drops sharply in the aquifer due to the high microbial electron-donor demand, driven by the presence of oxygen and nitrate. Outside of the zone of denitrification, the DOC concentration rises towards the groundwater boundary, driven by the hydrolysis of POC, reaching a maximum at about 1 m. The decreasing POC content away from the river yields a final gradual decline in DOC approaching the groundwater boundary.

3.1.3 Scenario BS: Bank Storage

In the bank storage scenario, the alternating inflow of nitrate from the aquifer and from the river leads to the formation of two distinct zones of denitrification (Figure 2, right column). The first one is located directly at the the river-aquifer interface. It is active only at the times when flow is from the river into the aquifer, hence supplying nitrate. We estimated the maximum penetration depth of the river water by integrating the positive part of the velocity function over one period. Via advection only, the water penetrates 0.23 m into the aquifer. Oxygen and nitrate reach that point only at very low concentrations because they are rapidly depleted after entering the aquifer.

The second zone of denitrification at about 1.1 m is fed by nitrate from the incoming groundwater. At the aquifer boundary, denitrification is mainly limited by carbon availability, such that nitrate concentrations remain at high values until the distance to the river is $x \approx 1.5$ m, after which they sharply decrease. Due to the flow reversal, this denitrification zone shifts between 1 m and 1.35 m over time. The response of concentrations to the

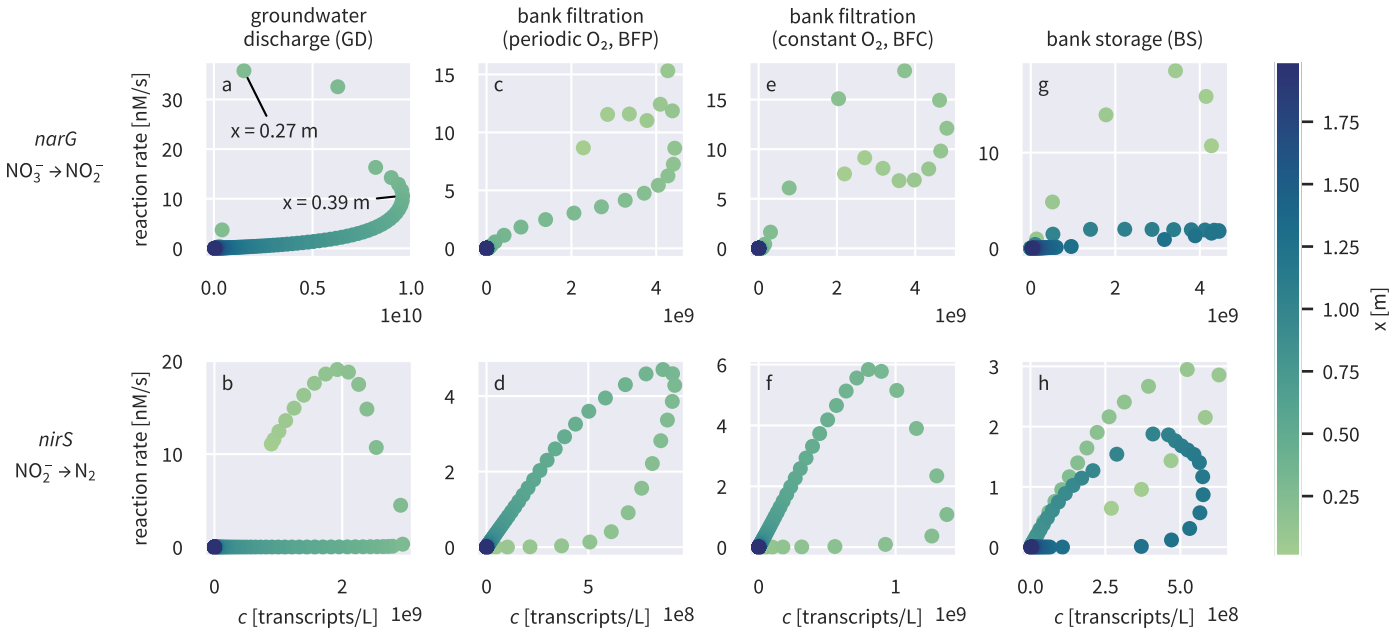

Figure 3. Relationships between the concentrations of functional-gene transcripts *narG* (upper row) and *nirS* (lower row) with the denitrification rates in the different scenarios. In the scenarios where concentrations do not reach constant steady state values but exhibit repeating diurnal cycles, daily averages of rates and concentrations are shown. The color indicates the spatial coordinate with dark blue corresponding to the groundwater inflow boundary and light green corresponding to the river boundary.

dynamic flow is generally similar to scenario BFP where the dynamics are caused by fluctuating oxygen concentrations. Both solute concentrations and mRNA strongly fluctuate over time while enzyme concentrations and biomass are stable because of their longer time scales of production and decay.

Compared to the other two scenarios, the DOC concentration in the bank storage scenario is high in the 1.2 m adjacent to the river. On average, the magnitude of the advective velocity and therefore the influx of electron acceptors (nitrate and oxygen) is smaller in this scenario. This limits the consumption of DOC and leads to its overall high concentration.

3.2 Relationship Between Transcripts/Enzymes and Reaction Rates

Based on our simulation results, we computed denitrification rates to explore how transcript and enzyme concentrations relate to the denitrification activity in the different scenarios (see Figure 3 for transcripts and Figure S4 for enzymes).

3.2.1 Scenario GD: Groundwater Discharge

In the groundwater-discharge scenario, the system reaches a steady state where the enzyme concentrations are proportional to transcript concentrations. Therefore, it is sufficient to analyze the relationship between reaction rates and transcripts *or* enzymes. For simplicity we compare rates to transcripts in Figure 3a and 3b. The relationships between rates and transcripts are non-linear and the correlation is positive in some parts of the domain, but negative or zero in other parts. At the groundwater-inflow boundary (dark blue colors), both *narG* transcript concentrations and NO_3^- reduction rates are close to zero and

increase towards the river (lighter colors). However, when the rates reach 10 nmol L^{-1} s^{-1} at 0.39 m, the trend reverses, that is, where transcript levels decrease reaction rates increase and reach their maximum at 0.27 m. At the points closest to the river boundary, both the nitrate reduction rate and *narG* transcript levels return to zero, closing the hysteresis loop.

The concentrations of *nirS* transcripts rise between 1 m and 0.3 m (Figure 3b). However, their increase does not correspond to an increase in reaction rates, suggesting that under certain conditions, transcript concentrations and reaction rates may be completely decoupled. One may intuitively expect that increasing reaction rates would be accompanied by increasing transcript concentrations. However, the rise of reaction rates between 0.3 m and 0.17 m is concomitant with the opposite, a decrease in transcript concentrations. A positive correlation between *nirS* transcript concentrations and reaction rates is only observed in the 15 cm closest to the river. The strong non-linearity of the transcript-rate relationships (and partly negative correlations) can be explained by the limited availability of DOC over most of the domain (which in this scenario originates from the river and hydrolysis of POC). The latter limits denitrification, whereas transcript production is still triggered by the presence of nitrate and nitrite, irrespective of electron-donor availability.

3.2.2 Scenario BF: Bank Filtration

Figure 4a and 4c show the relationship between transcript concentrations and denitrification rates for scenario BFP (bank filtration with a fluctuating oxygen inflow concentration). Reaction rates and transcript concentrations (and, to a lesser extent, also enzyme concentrations) both fluctuate over the course of the day, but the signals have a phase shift. This leads to a hysteresis in the relationship between transcript concentrations and reaction rates, with a different hysteretic pattern at different locations. Overall, transcript concentrations and denitrification rates do not show a clear (linear) relationship. These results suggest that it may not be possible to infer the denitrification activity at a given time and location from a single determination of the transcript concentration.

The relationship between enzyme concentrations and denitrification rates (Figure 4b, 4d) is also highly non-linear and location-specific. However, it exhibits less pronounced hysteresis loops because, in contrast to transcripts, the characteristic times for enzyme production and decay are longer than the time scale of the fluctuations. As a consequence, in dynamic steady state with diurnal cycles, the enzyme concentrations remain almost constant throughout the day, whereas the reaction rates fluctuate in response to the periodic concentration changes of aqueous substrates. Thus enzyme distributions could, under the right conditions, be used as proxies for delineating the average denitrification activity.

For the mitigation of nitrate contamination in groundwater daily averages of reaction rates are of greater interest than their diurnal fluctuations. To investigate whether repeated transcript measurements could be used as indicators of denitrification activity, we compare the daily averages of the denitrification rates and the transcript concentrations in Figures 3c and 3d. As can be seen, upon averaging more distinct positive correlations emerge, although they are still non-unique, particularly in the case of *nirS* transcripts, where the same transcript concentration can be associated with rates that differ by more than one order of magnitude. Different combinations of nitrite, oxygen and DOC concentrations can lead to the same transcript concentration, while the factors describing substrate limitation and oxygen inhibition affecting denitrification rates differ. The relationship looks very similar for transcripts and enzymes because daily averages of transcript concentrations are almost proportional to enzyme concentrations (see Figure S2).

The relationship between steady-state transcript concentrations and denitrification rates for BFC (bank filtration with constant oxygen input; Figure 3e, 3f) slightly differs from the BFP scenario (Figure 3c, 3d) but essentially mirrors the BFP characteristic features. For example, both bank filtration scenarios yield a positive, but non-unique, relationship of narG transcripts with the rates, whereas *nirS* transcripts exhibit a strong hysteretic behavior. It

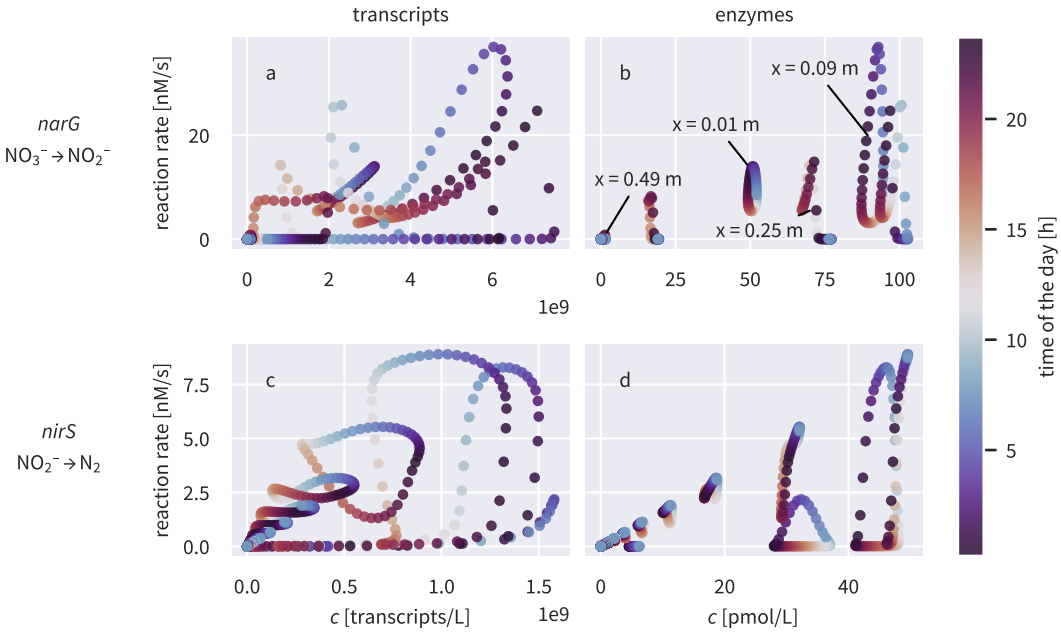

Figure 4. Relationships between transcript (left column) respectively enzyme (right column) concentrations and denitrification rates for scenario BFP (river water with fluctuating oxygen concentrations infiltrating groundwater). Colors indicate the time point within the diurnal cycle. Every location shows a distinct pattern (with one "loop" corresponding to one location), and many of them are non-linear and hysteretic in time.

is to be expected that the relationships are generally similar for the steady-state solution and daily averages of the periodic solution as the simulated concentration profiles are nearly the same in both cases (Figure 2, center), but non-linearity in the rate laws can lead to the observed differences.

3.2.3 Scenario BS: Bank Storage

Similar to the BFP scenario, the periodic reversal of flow in the BS scenario results in complex relationships between the transcript or enzyme concentrations and the denitrification rates (Figure S3). However, in contrast to BFP, daily averages of transcript concentrations and reaction rates (Figure 3g and 3h) show two clearly distinct patterns, corresponding to the two denitrification zones, and resembling to some extent the patterns of the pure groundwater-discharge and pure bank-filtration scenarios. In both zones, the relationships are non-linear and non-unique, analogous to all other scenarios. This is most evident for the *narG* transcripts (shown in Figure 3d).

3.3 Unraveling the Relationship Between Transcript Concentrations and Reaction Rates

The relationships between transcript concentrations and denitrification reaction rates, presented in the previous section, clearly show that transcript concentrations are not a reliable predictor of denitrification rates, even in cases where these are proportional to enzyme concentrations. Deviations from an expected linear relationship arise because denitrification rates are not only limited by enzyme concentrations (which, in turn, are ultimately deter-

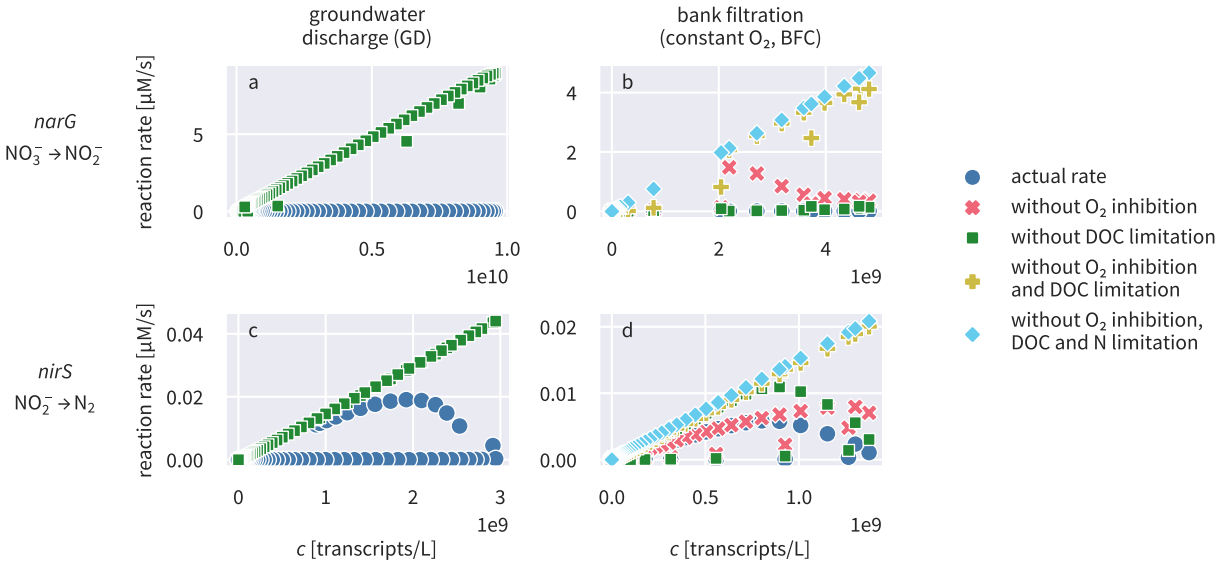

Figure 5. Relationship between the concentrations of functional-gene transcripts *narG* (upper row) and *nirS* (lower row) with potential denitrification rates after removing the effects of O_2 inhibition, DOC limitation, nitrogen substrate limitation, or combinations thereof. (Note: Scenarios where concentrations do not reach a steady state are omitted because correcting for the rate limitations based on time-averaged concentrations is not a valid approach).

mined by the nitrogen species triggering transcription), but also by substrate availability (in our study DOC and nitrogen species) and oxygen inhibition. In the model, we can eliminate these limitations by dividing the rate by the corresponding Michaelis-Menten or inhibition term. This then yields the potential denitrification rates. When these potential rates are compared to the transcript concentrations, clear positive relationships emerge (Figure 5).

In the groundwater-discharge scenario (Figure 5a, 5c), removing the DOC limitation yields a nearly linear relationship, showing that carbon limitation is the most important rate-limiting factor in this scenario. The remaining non-linearity of *narG*-transcripts at low reaction rates can be explained by the presence of nitrite near the river boundary, triggering *narG*-transcription even though nitrate levels and thus nitrate-removal rates are low.

The current model assumes that transcription of the denitrification genes is independent of DOC availability. While this approach is consistent with the current understanding of the targeted regulation of denitrification genes by nitrogen species and oxygen (Gaimster et al., 2018), our model formulation neglects unspecific mechanisms of gene regulation that act to shut down microbial metabolism at low carbon availability, thereby affecting denitrification genes. Accounting for transcription down-regulation of the denitrification genes under carbon limitation in our model formulation would likely yield relationships between transcripts and reaction rates closer to the potential rates without DOC limitation (Figure 5). Non-linear effects of DOC limitation on the reaction rates would persist. However, the absolute deviation from a linear relationship would be negligible when transcript concentrations and, therefore, potential rates are close to zero. Under extreme electron-donor limitation, our model predicts very low absolute transcript concentrations even without explicitly accounting for DOC-controlled down-regulation of transcription because DOC-limitation restricts microbial growth, leading to low biomass and, thereby, low transcript concentrations. However, if there is evidence for a large abundance of inactive denitrifiers, the model might need

to distinguish between the active and an inactive microbial pool, in which transcription is shut off (see, e.g., Chavez Rodriguez et al., 2020).

In the case of bank filtration with a constant oxygen concentration (Figure 5b, 5d), accounting for the DOC limitation term alone does not remove the non-linearity because oxygen inhibition also exerts an important control on denitrification. Eliminating both DOC limitation and oxygen inhibition leads to an approximately linear relationship between transcripts and potential rates. However, the corrected rates are orders of magnitude larger than the actual reaction rates.

In the scenarios in which concentrations undergo periodic fluctuations in time (BFP and BS), applying the correction terms would only be permissible for the time-variable rates and concentrations, but not for the averages. This is so because the correction terms are nonlinear and the concentrations involved are strongly correlated in time. Under such conditions, the product of their time-averaged values is not the same as the time-average of their product. Hence, applying corrections to the time-averaged rates to obtain a more unique relationship of the time-averaged transcript concentrations is not permissible. Similar effects have been described for spatial correlations of degrader communities and substrate concentrations in carbon cycling models. Chakrawal et al. (2020) used scale-transition theory to analyze how spatial correlations among state variables or between state variables and kinetic parameters affect upscaled reaction rates. In theory, the same method could be applied to obtain time-averaged rates based on average concentrations. However, it requires knowing the covariance terms of substrate and enzyme concentrations in time, which is not possible in practice because highly time-resolved measurements of transcript or substrate (DOC, nitrogen species) concentrations in groundwater are not available in the first place.

3.4 Implications for the Design of Field Sampling and Measurements

Our simulations show that transcripts of denitrification genes respond to short-term (diurnal) fluctuations of electron-acceptor concentrations, yielding highly temporally variable transcript concentrations at the river–groundwater interface. In such a dynamic system, analyses based on transcripts of functional genes would strongly depend on the time point of sampling. Transcripts exhibiting a low, even undetectable, abundance at a given time, may be present at much higher concentrations at other times of the day, and vice versa. Hence, interpretations on overall system behavior based on transcript concentrations obtained from sporadic sampling events, could be misleading in highly dynamic biogeochemical environments such as those found at the river–groundwater interface.

Based on our modeling results we simulated transcript measurements over time and space to illustrate, how different sampling frequencies and times can affect the outcome captured by measurement campaigns. Figure 6a shows time series of *nirS* transcript concentrations in the bank filtration scenario with fluctuating oxygen concentrations (BFP) at a distance of 0.17 m from the river, sampled at different frequencies (weekly samples, daily samples, 3 and 10 samples per day). We added a small random time perturbation to the sampling times to represent a realistic situation. The high sampling frequency of 10 samples per day captures the diurnal signal quite well. Taking 3 samples per day also captures the dynamic behavior of the system, albeit with less accuracy, with many of the peaks cut off and a more irregular signal than it actually is. Daily and weekly sampling creates apparent patterns in the data that are not linked to any real process but that are due to sampling the diurnal signal at slightly different times each day or week.

Figure 6b shows a spatial profile of simulated transcript measurements, taken at two different times of the day. While the general shape of the two profiles is similar, the location of the peak is shifted by about 10 cm, and between 5 cm and 20 cm the concentrations between the two time points differ by up to two orders of magnitude. This example emphasizes the need to consider the relevant time scale of variation for transcripts when planning

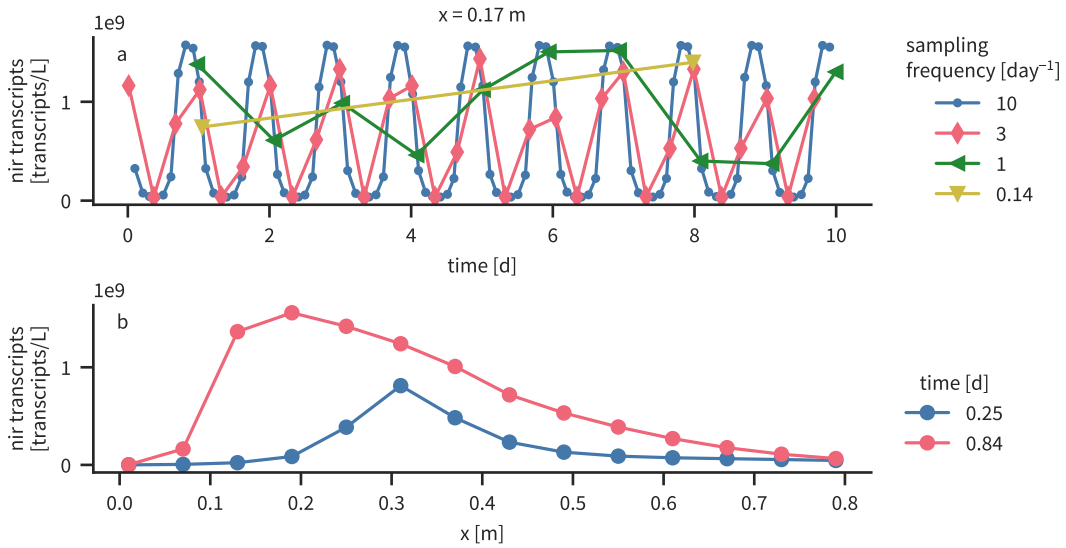

Figure 6. Simulated measurements of the *nirS* transcript concentrations. a) Effect of different sampling frequencies on a time series measured at a fixed location ($x = 0.17$ m). b) Dependence of a spatial profile on the time of the measurement.

measurement campaigns. Simple tools like redox- or oxygen-sensitive probes could provide a first approximation of what the relevant time scale for transcript dynamics is.

In contrast to transcripts, the concentrations of functional enzymes and functional biomass (which can be estimated by functional-gene concentrations) are much more dampened and hardly respond to diurnal fluctuations of electron-acceptor availability because of their larger time scales of production and decay. As a consequence, DNA-based methods such as the quantification of functional genes or metagenomics can provide information less dependent on short-term fluctuations of electron acceptor or electron-donor concentrations. However, a DNA-based approach, analogous to an enzyme-based approach, is subject to other uncertainties related to DNA's persistence and presence outside of active organisms (relic DNA) that can distort the characterization of the microbial community (Carini et al., 2016; Nielsen et al., 2007; Lennon et al., 2018), an effect not considered in this study. Different approaches to filter out the signals from relic DNA (viability PCR, e.g. Fittipaldi et al., 2012; Carini et al., 2016) and inactive microbes (BONCAT-FACS, selecting for translationally active cells, e.g. Couradeau et al., 2019) have been developed in the past years but are not yet applied routinely.

The unresponsiveness of enzyme concentrations and biomass in a system with short-term dynamics also implies that incorporating their time-variability into a biogeochemical model is not necessary and they can be assumed to be constant in time (i.e., via a biomass-implicit rate formulation). However, spatial variations should be considered, for example by using spatially variable rate coefficients. In systems in which the concentrations of electron acceptors vary over larger time scales (seasonal dynamics, flood events with effects of several days), the temporal variability of functional biomass and particularly enzyme concentrations might also play a role. Measurements of functional enzymes would also provide a more robust picture of microbial activity compared to functional-gene transcripts. Unfortunately, the quantification of functional enzymes (as opposed to transcripts) is not yet an established measurement technique for environmental samples, even though some pioneering studies have been done (e.g., Li et al., 2017).

Daily averaged transcript concentrations, however, are proportional to enzyme concentrations (for the scenarios investigated here), thus implying that several transcript measurements in time could replace the more difficult to measure enzymes in groundwater systems. Because only averages are required, mixing samples from several time points prior to RNA extraction could also help to reduce transcript measurement efforts. The main challenge, however, lies in obtaining samples from the same location at several time points, as sampling for gene quantification is destructive. When reactions are much slower than advective transport (low Damköhler number), several samples along a flowpath at a single time point (representing water parcels infiltrated at different times) could replace samples from the same location at several time points. In our simulations, however, reactions deplete substrates within a few centimeters. Water parcels with a time difference of 12 h are separated by a distance of 0.43 m, such that averaging over the locations does not provide a replacement for the temporal average at a single location. Therefore, samples should be taken at adjacent locations, corresponding to the same distance along a flow path (heterogeneity would make that more difficult). The latter illustrates the difficulty of acquiring time-resolved field measurements of transcripts. However, column experiments in the laboratory that simulate conditions in the field (see, e.g., Liu et al., 2017) provide a potential alternative, and would be a useful addition to capture higher-resolution dynamics.

Even after time-averaging, transcript or enzyme concentrations are not reliable predictors of reactions rates. The relationships in the simulated scenarios are non-unique and non-linear. Our analysis reveals that enzyme concentrations can be interpreted as a proxy for *potential* rates, which are hypothetical rates in the absence of specific limitations, such as substrate limitation and oxygen inhibition. These limitations reduce the potential rates towards the *actual* (in-situ) reaction rates.

Based on these findings we postulate an approach of how transcript or enzyme data could be used to directly predict denitrification rates. As a first step, the relationship between transcript concentrations and potential reaction rates needs to be determined. This could be achieved with lab incubations under non-limiting conditions. A caveat here is that under non-limiting conditions, a different part of the microbial community with a different physiology might be more active than under in-situ conditions (Hazard et al., 2021), modifying the relationship . In a system at steady state the relationship between transcript concentrations and potential reaction rates should ideally be linear. Measured transcript concentrations can subsequently serve as a predictor of potential rates which then need to be amended by rate limiting factors like substrate limitation to obtain the actual reaction rates. This correction step does not only require measurements of the involved solute concentrations, but also estimates of parameters describing rate-limiting factors of reaction kinetics (half-saturation and inhibition constants). Such parameter values are often not well known and reported values typically range over several orders of magnitude (see, e.g., García-Ruiz et al., 1998). Therefore, additional experiments to determine specific parameters of the studied system would be necessary.

A powerful integrative approach would be to use a process-based reactive-transport model to predict reaction rates, making use of molecular-biological data to determine model parameters. One advantage is that once a process-based model is calibrated it can deliver reaction rates at time-points and locations where no data are available. We therefore suggest the following strategy combining molecular biological data, biogeochemical measurements and modeling to determine denitrification rates.

1. *Measure functional enzymes, genes or transcripts to determine temporally stable, spatial profiles of the active functional biomass.* Our simulations show that profiles of daily averaged transcript concentrations, enzymes, and functional biomass are very similar and generally linked to the denitrification activity. Given the challenges of measuring time-averages of transcript concentrations and excluding inactive biomass in DNA-based methods, enzyme measurements seem to be the most accurate proxy variable for

active functional biomass. These data will provide a relative measure of the spatially variable maximum rate coefficient in a biomass-implicit rate formulation. Compared to an enzyme-explicit formulation (as used in this study), a biomass-implicit formulation has the advantage that it requires fewer parameters. The hypothesis that the active functional biomass maintains a constant spatial distribution should be verified with repeated measurements at different time points, and seasonal trends could potentially be accounted for using several coefficients. If a considerable time-variability of active functional biomass is observed, a biomass- or enzyme-explicit model formulation that provides a process-based explanation for the variability should replace the biomass-implicit formulation.

2. *Measure oxygen, nitrogen substrates and DOC at several locations with a high temporal resolution.* These data are required to appropriately account for substrate limitations and oxygen inhibition. In order to capture the short-term variability inherent to these variables, continuous logging with probes, if possible, is a good approach (e.g., for oxygen). Otherwise, manual measurements should also cover several temporal scales. For example, hourly measurements that capture diurnal dynamics on individual days could be combined with daily or weekly samples to provide information about longer terms dynamics.
3. *Use a process-based model to obtain temporally and spatially resolved predictions of concentrations and reaction rates.* The model integrates the different data types through the calibration of model parameters, yielding estimates of total in-situ denitrification rates, that are otherwise impossible to obtain with direct measurements.

The predictions of a reactive-transport model strongly depend on transport related parameters, such as flow velocities or solute fluxes at boundaries, governed by subsurface hydraulic conductivity. Therefore, at field sites, complementary hydrogeological data should accompany biogeochemical investigations.

3.5 Conclusions and Outlook

Our simulations highlight some of the prospects and limitations of using functional-gene transcripts and enzymes to characterize biogeochemical reactions at the river–groundwater interface. Concentrations of functional-gene transcripts quickly respond to changes in substrate concentrations and oxygen levels, implying that dynamic systems need to be sampled at the appropriate temporal resolution. High transcript and enzyme concentrations spatially coincide with active denitrification and are therefore qualitative indicators of reactive zones. Substrate limitation and oxygen inhibition of the enzymes, however, impede quantitative predictions of reaction rates from transcript or enzyme concentrations.

We based our study on a relatively simple model that describes only a part of the system (gene regulation of denitrification) in detail, with the advantage that it enables a straightforward analysis of predicted patterns. However, even with our simplistic model formulation, the relationships between transcript or enzyme concentrations and denitrification rates are not straightforward. Our results highlight that a rigorous quantitative interpretation of transcript or enzyme data is not possible without a process-based mathematical model. While our purely numerical study provides predictions of expected transcript and enzyme behavior in dynamic natural systems, it does not replace laboratory and field investigations. In fact, we highlight that further improvements in enzyme-explicit model development will depend on highly-temporally resolved measurement campaigns.

Further, highly spatially resolved measurements are also needed to capture the biogeochemical reactivity of heterogeneous subsurface environments. Subsurface lithofacies of varying physical and chemical properties yield transitions between more permeable, oxidized, and less permeable, reducing zones, with greater availability of electron donors. Reaction rates are highest at the interfaces between the facies where electron donors and acceptors meet (Sawyer, 2015; Stegen et al., 2016). We expect that in such heterogeneous

subsurface environments, transcripts and enzymes related to denitrification would also be non-uniformly distributed and, hence, sampling a single location carries the risk that the measured functional potential is not representative for the system as a whole. Additionally, the correction approach for potential rates would not be easily applicable, because spatial correlations of enzyme and substrate concentrations lead to different effective rate laws (Chakrawal et al., 2020).

In natural systems, other N-cycling processes (nitrification, anaerobic ammonium oxidation (annamox), dissimilatory nitrate reduction to ammonium (DNRA)), alternative electron donors (e.g., reduced sulfur and iron species/minerals), and the temperature dependence of the reaction kinetics can also affect denitrification rates. In a next step of model development, further nitrogen cycling processes, in particular nitrification and DNRA, should be included into models to better represent the functional potential of natural microbial communities. Instead of simulating microbial biomass as a single variable, a model that considers more N-cycling processes should use a gene-centric approach (Reed et al., 2014) to account for the fact that the reactions are carried out by different organisms.

Acronyms

BDF Backwards Differentiation Formula
DNRA Dissimilatory nitrate reduction to ammonium
DOC Dissolved organic carbon
NAR Nitrate reductase
NIR Nitrite reductase
ODE Ordinary differential equation
POC Particulate organic carbon

Open Research

Version 0.1.0 of the Python package Nitrogene (Störiko et al., 2021b) used for defining the reaction model and analyzing output data is preserved at `https://doi.org/10.5281/zenodo.5590919`, available under an MIT license and developed openly at `https://gitlab.com/astoeriko/nitrogene`. The repository also contains the output data used to generate figures.

Version 0.1.0 of the Python package adrpy (Störiko, 2021) used for coupling the reactions to 1-D advective-dispersive transport is preserved at `https://doi.org/10.5281/zenodo.5590973`, available under an MIT license and developed openly at `https://gitlab.com/astoeriko/adrpy`.

Version 0.2.2 of the Sunode library (Seyboldt, 2021) used to solve the ODEs resulting from spatial discretization of the advection-dispersion-reaction equation is preserved at `https://doi.org/10.5281/zenodo.5213947`, available under an MIT license and developed openly at `https://github.com/aseyboldt/sunode`.

Acknowledgments

This work was funded by the German Research Foundation (DFG) within the Research Training Group RTG 1829 Integrated Hydrosystem Modelling (DFG Grant agreement GRK 1829) and the Collaborative Research Center CRC 1253 CAMPOS–Catchments as Reactors, project P7 (DFG Grant agreement SFB 1253/1).

References

Akbarzadeh, Z., Laverman, A. M., Rezanezhad, F., Raimonet, M., Viollier, E., Shafei, B., &

Van Cappellen, P. (2018, July). Benthic nitrite exchanges in the Seine River (France): An early diagenetic modeling analysis. *Science of The Total Environment*, *628–629*, 580–593. doi: 10.1016/j.scitotenv.2018.01.319

Bernstein, J. A., Khodursky, A. B., Lin, P.-H., Lin-Chao, S., & Cohen, S. N. (2002, July). Global analysis of mRNA decay and abundance in *Escherichia coli* at single-gene resolution using two-color fluorescent DNA microarrays. *Proceedings of the National Academy of Sciences of the United States of America*, *99*(15), 9697–9702. doi: 10.1073/pnas.112318199

Bertin, C., & Bourg, A. C. M. (1994, May). Radon-222 and chloride as natural tracers of the infiltration of river water into an alluvial aquifer in which there is significant river/groundwater mixing. *Environmental Science & Technology*, *28*(5), 794–798. doi: 10.1021/es00054a008

Bol, R., Lücke, A., Tappe, W., Kummer, S., Krause, M., Weigand, S., … Vereecken, H. (2015). Spatio-temporal variations of dissolved organic matter in a German forested mountainous headwater catchment. *Vadose Zone Journal*, *14*(4), vzj2015.01.0005. doi: 10.2136/vzj2015.01.0005

Brow, C. N., O'Brien Johnson, R., Johnson, R. L., & Simon, H. M. (2013, September). Assessment of anaerobic toluene biodegradation activity by *bssA* transcript/gene ratios. *Applied and Environmental Microbiology*, *79*(17), 5338–5344. doi: 10.1128/AEM.01031-13

Carini, P., Marsden, P. J., Leff, J. W., Morgan, E. E., Strickland, M. S., & Fierer, N. (2016, December). Relic DNA is abundant in soil and obscures estimates of soil microbial diversity. *Nature Microbiology*, *2*(3), 1–6. doi: 10.1038/nmicrobiol.2016.242

Chakrawal, A., Herrmann, A. M., Koestel, J., Jarsjö, J., Nunan, N., Kätterer, T., & Manzoni, S. (2020, March). Dynamic upscaling of decomposition kinetics for carbon cycling models. *Geoscientific Model Development*, *13*(3), 1399–1429. doi: 10.5194/gmd-13-1399-2020

Chavez Rodriguez, L., Ingalls, B., Schwarz, E., Streck, T., Uksa, M., & Pagel, H. (2020, November). Gene-centric model approaches for accurate prediction of pesticide biodegradation in soils. *Environmental Science & Technology*, *54*(21), 13638–13650. doi: 10.1021/acs.est.0c03315

Couradeau, E., Sasse, J., Goudeau, D., Nath, N., Hazen, T. C., Bowen, B. P., … Northen, T. R. (2019, June). Probing the active fraction of soil microbiomes using BONCAT-FACS. *Nature Communications*, *10*(1), 2770. doi: 10.1038/s41467-019-10542-0

Danczak, R. E., Sawyer, A. H., Williams, K. H., Stegen, J. C., Hobson, C., & Wilkins, M. J. (2016). Seasonal hyporheic dynamics control coupled microbiology and geochemistry in Colorado River sediments. *Journal of Geophysical Research: Biogeosciences*, *121*(12), 2976–2987. doi: 10.1002/2016JG003527

Ding, D. (2010, May). Transport of bacteria in aquifer sediment: Experiments and modeling. *Hydrogeology Journal*, *18*(3), 669–679. doi: 10.1007/s10040-009-0559-3

Erisman, J. W., Galloway, J. N., Seitzinger, S., Bleeker, A., Dise, N. B., Petrescu, A. M. R., … de Vries, W. (2013, July). Consequences of human modification of the global nitrogen cycle. *Philosophical Transactions of the Royal Society B: Biological Sciences*, *368*(1621), 20130116. doi: 10.1098/rstb.2013.0116

Fittipaldi, M., Nocker, A., & Codony, F. (2012, November). Progress in understanding preferential detection of live cells using viability dyes in combination with DNA amplification. *Journal of Microbiological Methods*, *91*(2), 276–289. doi: 10.1016/j.mimet.2012.08.007

Gaimster, H., Alston, M., Richardson, D. J., Gates, A. J., & Rowley, G. (2018, March). Transcriptional and environmental control of bacterial denitrification and N_2O emissions. *FEMS Microbiology Letters*, *365*(5). doi: 10.1093/femsle/fnx277

García-Ruiz, R., Pattinson, S. N., & Whitton, B. A. (1998, July). Kinetic parameters of denitrification in a river continuum. *Applied and Environmental Microbiology*, *64*(7), 2533–2538. doi: 10.1128/AEM.64.7.2533-2538.1998

Gelhar, L. W., Welty, C., & Rehfeldt, K. R. (1992). A critical review of data on field-scale

dispersion in aquifers. *Water Resources Research*, *28*(7), 1955–1974. doi: 10.1029/92WR00607

Gerecht, K. E., Cardenas, M. B., Guswa, A. J., Sawyer, A. H., Nowinski, J. D., & Swanson, T. E. (2011). Dynamics of hyporheic flow and heat transport across a bed-to-bank continuum in a large regulated river. *Water Resources Research*, *47*(3). doi: 10.1029/2010WR009794

Griebler, C., Mindl, B., Slezak, D., & Geiger-Kaiser, M. (2002, June). Distribution patterns of attached and suspended bacteria in pristine and contaminated shallow aquifers studied with an in situ sediment exposure microcosm. *Aquatic Microbial Ecology*, *28*(2), 117–129. doi: 10.3354/ame028117

Grösbacher, M., Eckert, D., Cirpka, O. A., & Griebler, C. (2018, June). Contaminant concentration versus flow velocity: Drivers of biodegradation and microbial growth in groundwater model systems. *Biodegradation*, *29*(3), 211–232. doi: 10.1007/s10532-018-9824-2

Gu, C., Hornberger, G. M., Mills, A. L., Herman, J. S., & Flewelling, S. A. (2007, December). Nitrate reduction in streambed sediments: Effects of flow and biogeochemical kinetics. *Water Resources Research*, *43*(12). doi: 10.1029/2007WR006027

Härtig, E., & Zumft, W. G. (1999, January). Kinetics of *nirS* expression (cytochrome cd_1 nitrite reductase) in *Pseudomonas stutzeri* during the transition from aerobic respiration to denitrification: Evidence for a denitrification-specific nitrate- and nitrite-responsive regulatory system. *Journal of Bacteriology*, *181*(1), 161–166. doi: 10.1128/JB.181.1.161-166.1999

Harvey, J. W., Böhlke, J. K., Voytek, M. A., Scott, D., & Tobias, C. R. (2013). Hyporheic zone denitrification: Controls on effective reaction depth and contribution to whole-stream mass balance. *Water Resources Research*, *49*(10), 6298–6316. doi: 10.1002/wrcr.20492

Hassan, J., Bergaust, L. L., Wheat, I. D., & Bakken, L. R. (2014, November). Low probability of initiating *nirS* transcription explains observed gas kinetics and growth of bacteria switching from aerobic respiration to denitrification. *PLoS Computational Biology*, *10*(11), e1003933. doi: 10.1371/journal.pcbi.1003933

Hassan, J., Qu, Z., Bergaust, L. L., & Bakken, L. R. (2016, January). Transient accumulation of NO_2^- and N_2O during denitrification explained by assuming cell diversification by stochastic transcription of denitrification genes. *PLoS Computational Biology*, *12*(1). doi: 10.1371/journal.pcbi.1004621

Hayashi, M., Vogt, T., Mächler, L., & Schirmer, M. (2012, July). Diurnal fluctuations of electrical conductivity in a pre-alpine river: Effects of photosynthesis and groundwater exchange. *Journal of Hydrology*, *450–451*, 93–104. doi: 10.1016/j.jhydrol.2012.05.020

Hazard, C., Prosser, J. I., & Nicol, G. W. (2021, June). Use and abuse of potential rates in soil microbiology. *Soil Biology and Biochemistry*, *157*, 108242. doi: 10.1016/j.soilbio.2021.108242

Hindmarsh, A. C., Brown, P. N., Grant, K. E., Lee, S. L., Serban, R., Shumaker, D. E., & Woodward, C. S. (2005). SUNDIALS: Suite of nonlinear and differential/algebraic equation solvers. *ACM Transactions on Mathematical Software (TOMS)*, *31*(3), 363–396. doi: 10.1145/1089014.1089020

Kennedy, C. D., Genereux, D. P., Corbett, D. R., & Mitasova, H. (2009). Spatial and temporal dynamics of coupled groundwater and nitrogen fluxes through a streambed in an agricultural watershed. *Water Resources Research*, *45*(9). doi: 10.1029/2008WR007397

Kinzelbach, W., Schäfer, W., & Herzer, J. (1991, June). Numerical modeling of natural and enhanced denitrification processes in aquifers. *Water Resources Research*, *27*(6), 1123–1135. doi: 10.1029/91WR00474

Knights, D., Sawyer, A. H., Barnes, R. T., Musial, C. T., & Bray, S. (2017). Tidal controls on riverbed denitrification along a tidal freshwater zone. *Water Resources Research*, *53*(1), 799–816. doi: 10.1002/2016WR019405

Krause, S., Hannah, D. M., Fleckenstein, J. H., Heppell, C. M., Kaeser, D., Pickup, R., … Wood, P. J. (2011). Inter-disciplinary perspectives on processes in the hyporheic

zone. *Ecohydrology*, *4*(4), 481–499. doi: 10.1002/eco.176

Krause, S., Lewandowski, J., Grimm, N. B., Hannah, D. M., Pinay, G., McDonald, K., … Turk, V. (2017). Ecohydrological interfaces as hot spots of ecosystem processes. *Water Resources Research*, *53*(8), 6359–6376. doi: 10.1002/2016WR019516

Kunz, J. V., Hensley, R., Brase, L., Borchardt, D., & Rode, M. (2017). High frequency measurements of reach scale nitrogen uptake in a fourth order river with contrasting hydromorphology and variable water chemistry (Weiße Elster, Germany). *Water Resources Research*, *53*(1), 328–343. doi: 10.1002/2016WR019355

Kuypers, M. M. M., Marchant, H. K., & Kartal, B. (2018, May). The microbial nitrogen-cycling network. *Nature Reviews Microbiology*, *16*(5), 263–276. doi: 10.1038/nrmicro.2018.9

Lennon, J. T., Muscarella, M. E., Placella, S. A., & Lehmkuhl, B. K. (2018, July). How, when, and where relic DNA affects microbial diversity. *mBio*, *9*(3). doi: 10.1128/mBio.00637-18

Li, M., Gao, Y., Qian, W.-J., Shi, L., Liu, Y., Nelson, W. C., … Liu, C. (2017). Targeted quantification of functional enzyme dynamics in environmental samples for microbially mediated biogeochemical processes. *Environmental Microbiology Reports*, *9*(5), 512–521. doi: 10.1111/1758-2229.12558

Liu, Y., Liu, C., Nelson, W. C., Shi, L., Xu, F., Liu, Y., … Zachara, J. M. (2017, May). Effect of water chemistry and hydrodynamics on nitrogen transformation activity and microbial community functional potential in hyporheic zone sediment columns. *Environmental Science & Technology*, *51*(9), 4877–4886. doi: 10.1021/acs.est.6b05018

Maier, T., Schmidt, A., Güell, M., Kühner, S., Gavin, A.-C., Aebersold, R., & Serrano, L. (2011, July). Quantification of mRNA and protein and integration with protein turnover in a bacterium. *Molecular Systems Biology*, *7*, 511. doi: 10.1038/msb.2011.38

Mailloux, B. J., & Fuller, M. E. (2003, July). Determination of in situ bacterial growth rates in aquifers and aquifer sediments. *Applied and Environmental Microbiology*, *69*(7), 3798–3808. doi: 10.1128/AEM.69.7.3798-3808.2003

Marmonier, P., Fontvieille, D., Gibert, J., & Vanek, V. (1995, September). Distribution of dissolved organic carbon and bacteria at the interface between the Rhône river and its alluvial aquifer. *Journal of the North American Benthological Society*, *14*(3), 382–392. doi: 10.2307/1467204

Mellage, A., Eckert, D., Grösbacher, M., Inan, A. Z., Cirpka, O. A., & Griebler, C. (2015, June). Dynamics of suspended and attached aerobic toluene degraders in small-scale flow-through sediment systems under growth and starvation conditions. *Environmental Science & Technology*, *49*(12), 7161–7169. doi: 10.1021/es5058538

Monard, C., Martin-Laurent, F., Lima, O., Devers-Lamrani, M., & Binet, F. (2013, April). Estimating the biodegradation of pesticide in soils by monitoring pesticide-degrading gene expression. *Biodegradation*, *24*(2), 203–213. doi: 10.1007/s10532-012-9574-5

Nielsen, K. M., Johnsen, P. J., Bensasson, D., & Daffonchio, D. (2007). Release and persistence of extracellular DNA in the environment. *Environmental Biosafety Research*, *6*(1-2), 37–53. doi: 10.1051/ebr:2007031

Qu, Z., Bakken, L. R., Molstad, L., Frostegård, Å., & Bergaust, L. L. (2015, November). Transcriptional and metabolic regulation of denitrification in *Paracoccus denitrificans* allows low but significant activity of nitrous oxide reductase under oxic conditions. *Environmental Microbiology*, *18*(9), 2951–2963. doi: 10.1111/1462-2920.13128

Rahm, B. G., & Richardson, R. E. (2008, July). Dehalococcoides' gene transcripts as quantitative bioindicators of tetrachloroethene, trichloroethene, and cis-1,2-dichloroethene dehalorespiration rates. *Environmental Science & Technology*, *42*(14), 5099–5105. doi: 10.1021/es702912t

Reed, D. C., Algar, C. K., Huber, J. A., & Dick, G. J. (2014, February). Gene-centric approach to integrating environmental genomics and biogeochemical models. *Proceedings of the National Academy of Sciences*, *111*(5), 1879–1884. doi: 10.1073/pnas.1313713111

Reid, T., Chaganti, S. R., Droppo, I. G., & Weisener, C. G. (2018, June). Novel insights into freshwater hydrocarbon-rich sediments using metatranscriptomics: Opening the

black box. *Water Research*, *136*, 1–11. doi: 10.1016/j.watres.2018.02.039

Rohe, L., Oppermann, T., Well, R., & Horn, M. A. (2020, December). Nitrite induced transcription of *p450nor* during denitrification by *Fusarium oxysporum* correlates with the production of N_2O with a high ^{15}N site preference. *Soil Biology and Biochemistry*, *151*, 108043. doi: 10.1016/j.soilbio.2020.108043

Sanz-Prat, A., Lu, C., Amos, R. T., Finkel, M., Blowes, D. W., & Cirpka, O. A. (2016, September). Exposure-time based modeling of nonlinear reactive transport in porous media subject to physical and geochemical heterogeneity. *Journal of Contaminant Hydrology*, *192*, 35–49. doi: 10.1016/j.jconhyd.2016.06.002

Sawyer, A. H. (2015). Enhanced removal of groundwater-borne nitrate in heterogeneous aquatic sediments. *Geophysical Research Letters*, *42*(2), 403–410. doi: 10.1002/2014GL062234

Sawyer, A. H., Cardenas, M. B., Bomar, A., & Mackey, M. (2009). Impact of dam operations on hyporheic exchange in the riparian zone of a regulated river. *Hydrological Processes*, *23*(15), 2129–2137. doi: 10.1002/hyp.7324

Scheidegger, A. E. (1974). *The physics of flow through porous media* (Third ed.). Toronto: University of Toronto Press. doi: 10.3138/9781487583750

Seyboldt, A. (2021, August). Sunode [Computer software]. Zenodo. doi: 10.5281/zenodo.5213947

Smith, H. J., Zelaya, A. J., De León, K. B., Chakraborty, R., Elias, D. A., Hazen, T. C., … Fields, M. W. (2018, September). Impact of hydrologic boundaries on microbial planktonic and biofilm communities in shallow terrestrial subsurface environments. *FEMS Microbiology Ecology*, *94*(12), fiy191. doi: 10.1093/femsec/fiy191

Stegen, J. C., Konopka, A., McKinley, J. P., Murray, C., Lin, X., Miller, M. D., … Fredrickson, J. K. (2016, September). Coupling among microbial communities, biogeochemistry and mineralogy across biogeochemical facies. *Scientific Reports*, *6*(1), 30553. doi: 10.1038/srep30553

Stelzer, R. S., Bartsch, L. A., Richardson, W. B., & Strauss, E. A. (2011, October). The dark side of the hyporheic zone: Depth profiles of nitrogen and its processing in stream sediments. *Freshwater Biology*, *56*(10), 2021–2033. doi: 10.1111/j.1365-2427.2011.02632.x

Stief, P., Beer, D., & Neumann, D. (2002, May). Small-scale distribution of interstitial nitrite in freshwater sediment microcosms: The role of nitrate and oxygen availability, and sediment permeability. *Microbial Ecology*, *43*(3), 367–377. doi: 10.1007/s00248-002-2008-x

Stoliker, D. L., Repert, D. A., Smith, R. L., Song, B., LeBlanc, D. R., McCobb, T. D., … Kent, D. B. (2016, April). Hydrologic controls on nitrogen cycling processes and functional gene abundance in sediments of a groundwater flow-through lake. *Environmental Science & Technology*, *50*(7), 3649–3657. doi: 10.1021/acs.est.5b06155

Störiko, A. (2021, October). Adrpy: Advection-Dispersion-Reaction models in Python [Computer software]. Zenodo. doi: 10.5281/zenodo.5590973

Störiko, A., Pagel, H., Mellage, A., & Cirpka, O. (2021b, October). Nitrogene: Modelling code and data of an enzyme-based denitrification model [Computer software]. Zenodo. doi: 10.5281/zenodo.5590919

Störiko, A., Pagel, H., Mellage, A., & Cirpka, O. A. (2021a). Does it pay off to explicitly link functional gene expression to denitrification rates in reaction models? *Frontiers in Microbiology*, *12*. doi: 10.3389/fmicb.2021.684146

Wang, S., Wang, W., Zhao, S., Wang, X., Hefting, M. M., Schwark, L., & Zhu, G. (2019, October). Anammox and denitrification separately dominate microbial N-loss in water saturated and unsaturated soils horizons of riparian zones. *Water Research*, *162*, 139–150. doi: 10.1016/j.watres.2019.06.052

Water Resources Research

Supporting Information for

Denitrification-driven transcription and enzyme production at the river–groundwater interface: Insights from reactive-transport modeling

Anna Störiko[1], Holger Pagel[2], Adrian Mellage[1], Philippe Van Cappellen[3], Olaf A. Cirpka[1]

[1] Center for Applied Geoscience, University of Tübingen, Tübingen, Germany
[2] Biogeophysics, Institute of Soil Science and Land Evaluation, University of Hohenheim, Stuttgart, Germany
[3] Water Institute, Department of Earth and Environmental Sciences, University of Waterloo, Waterloo, Ontario, Canada

Contents of this file

Introduction

The supporting information includes additional figures created from the model outputs.

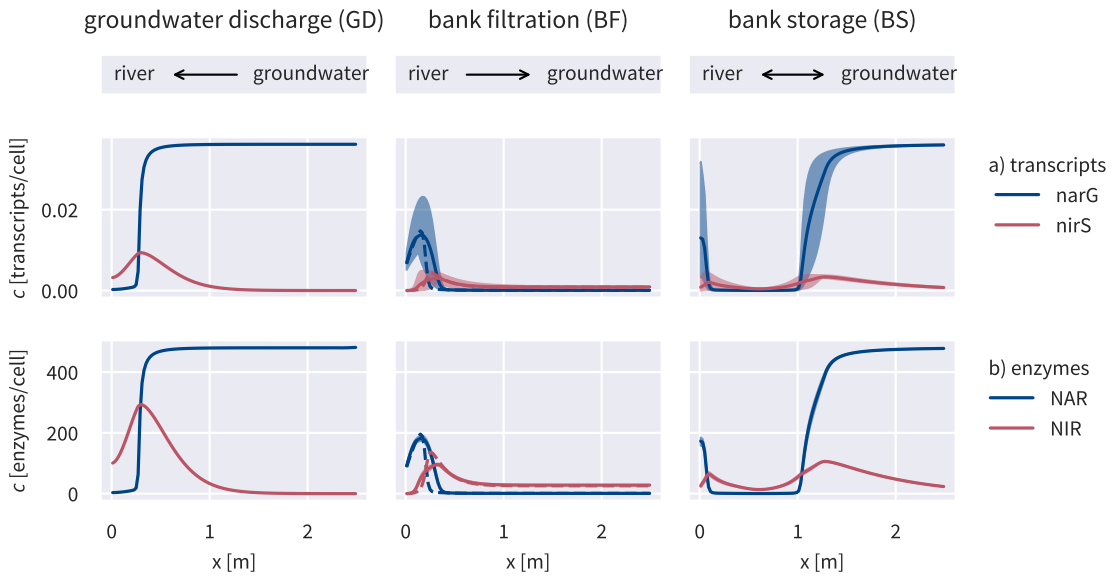

Figure S1: Spatial distributions of transcript and enzyme concentrations normalized by biomass. The steady-state solution in scenario BFC is indicated by a dashed line. For the periodic solution in scenarios BFP and BS, the minimum and maximum value over time are indicated by the shaded area, the mean value is plotted as a solid line. Concentrations between 2.5 m and the groundwater-side domain boundary at 4 m are omitted because they are almost constant.

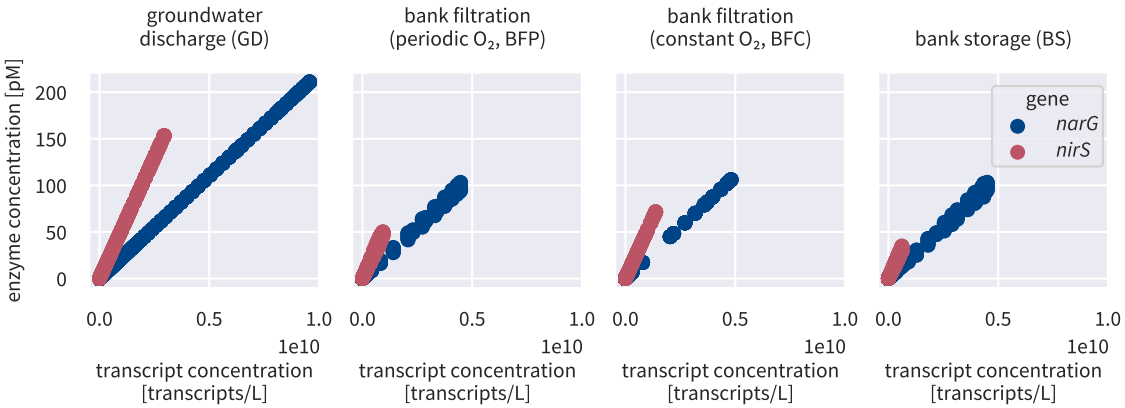

Figure S2: Relationships between transcript concentrations and enzyme concentrations. In scenarios GD and BFC, concentrations are at steady state. In scenarios BFP and BS, transcript concentrations, but not enzyme concentrations, are averaged over time.

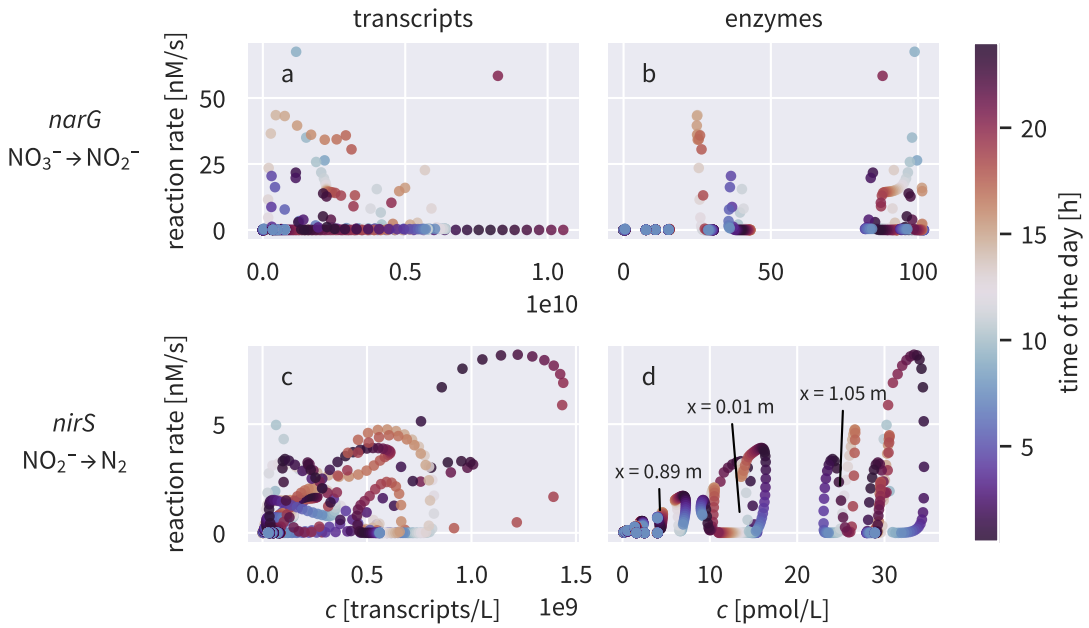

Figure S3: Relationships between transcript (left column) respectively enzyme (right column) concentrations and denitrification rates for the bank storage (BS) scenario. Colors indicate the time point within the diurnal cycle. Every location shows a distinct pattern (with one "loop" corresponding to one location), and many of them are non-linear and hysteretic in time.

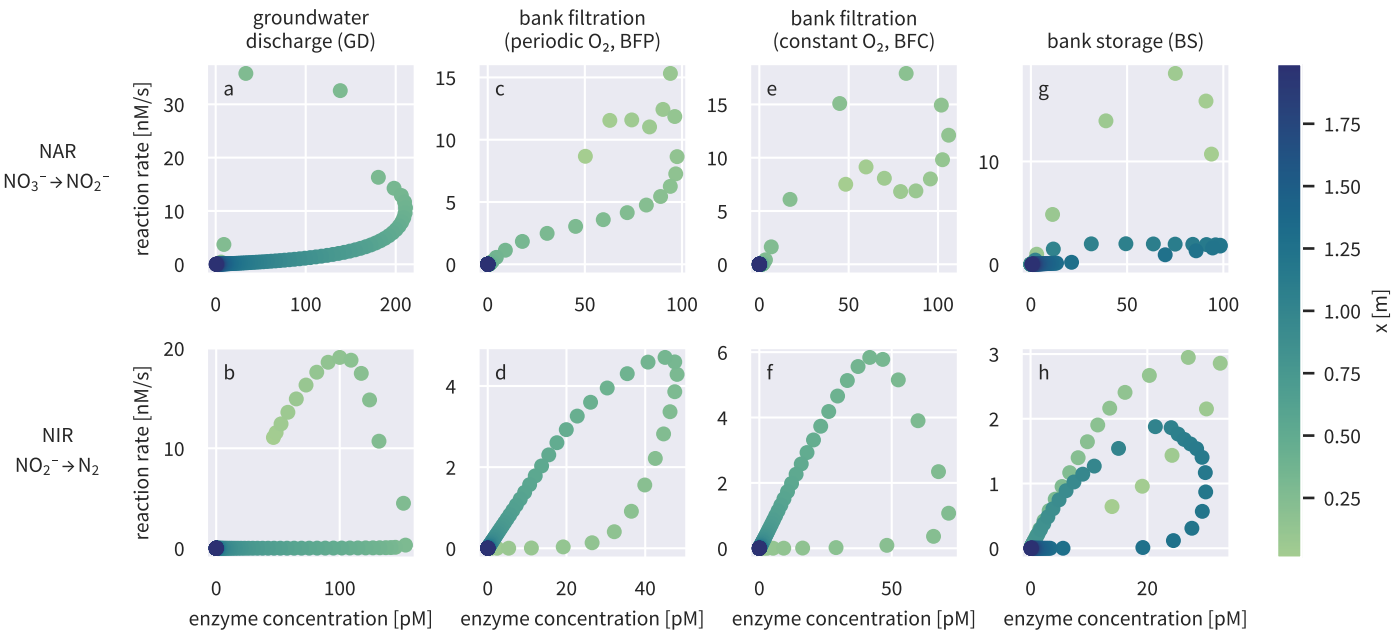

Figure S4: Relationships between the concentrations of enzymes NAR (upper row) and NIR (lower row) with the denitrification rates in the different scenarios. In the scenarios where concentrations do not reach a steady state but stable diurnal cycles, daily averages of rates and concentrations are shown. The color indicates the spatial coordinate with dark blue corresponding to the groundwater inflow boundary and light green corresponding to the river boundary.